SOME NOVEL APPLICATIONS OF POINT SOURCE AND POINT DETECTOR FOR ULTRASONIC WAVES

Kwang Yul Kim and Wolfgang Sachse

Department of Theoretical and Applied Mechanics, Thurston Hall
Cornell University, Ithaca, New York 14853

ABSTRACT

This paper describes some novel applications of point-like source and point-like detector for ultrasonic waves to the investigation of various physical phenomena, which we have recently carried out. The point-like sources are generated by the fracture of a glass capillary, a focused laser beam and small PZT transducers, while the point-like detectors include small PZT and capacitive transducers. The topics discussed are first, observation of focusing of fast transverse (FT) mode in silicon: second, determination of wave or group velocity surfaces of zinc, which include those of longitudinal (L), FT, and slow transverse (ST) waves, cuspidal features of the ST mode, and the head wave front: third, observation of a phenomenon related with the external conical refraction in zinc, i.e., the focusing of the ST mode toward the symmetry axis.

I. INTRODUCTION

Over the last decade the method of point source and point detector (PS/PD) has found increasing applications to the characterization of acoustic medium, emission source, and detector. These applications encompass such diverse areas as photoacoustics, fracture and fatigue, focusing of phonon and ultrasonic waves, wavespeed and dispersion relation, nondestructive inspection, and so forth. The point-like sources can be generated with the impact of small particles, fracture of tiny glass capillary and pencil lead, irradiation of focused laser and x-ray beams with very short duration, or excitation of small piezoelectric transducers. The point-like detectors are divided into contact and non-contact types. The former includes piezoelectric transducers, whereas laser interferometer [1] and small capacitive transducer belong to the latter. We have recently fabricated very small capacitive displacement transducers [2] and PZT transducers of both longitudinal and transverse modes, and successfully applied them to our research. The size of all these transducers is less than or equal to 1 mm in diameter. This paper deals with the results obtained by applying the PS/PD method to the single crystals of zinc and silicon, which are respectively oriented in the [0001] and [001] directions, for investigation of various physical phenomena to be described in the following sections. They are novel in the sense that to our knowledge these are the first observations of their kinds ever reported.

II. FOCUSING OF FAST TRANSVERSE MODE IN SILICON

Focusing of acoustic energy into certain directions of anisotropic crystals has been reported in the cases of ballistic phonons excited by a heat pulse generated in the crystal cooled to cryogenic temperatures [3], ultrasonic waves excited by a pulsed laser beam [4] and a focal longitudinal transducer immersed in a coupling fluid [5], and surface acoustic waves (SAW) excited by a pulsed laser beam [6]. These point-like sources of acoustic energy generate either a longitudinal mode only or coupled quasi longitudinal and slow quasi transverse (ST) waves of shear vertical (SV) polarization. The axisymmetric nature of these sources results in the absence of fast transverse (FT) mode of shear horizontal (SH) polarization, which is uncoupled from the other two modes. Therefore, the reported focusing of acoustic energy pertains either to the longitudinal mode or mostly to the ST mode whose slowness surface of an anisotropic medium shows in general convex or concave curvatures. The characteristics of these point-like sources inject their energy into every possible direction allowed by the medium.

Instead of axisymmetric sources, we used in our experiment two small PZT shear transducers attached on the surface of a [001]-oriented silicon, one transducer to generate FT waves and the other to detect them on the side opposite to the source's. The polarization of both transducers were aligned in the [100] direction of the sample which was 49.15 mm thick and 100 mm in diameter. The detectors were scanned along the [100] direction on the surface across three spots which were located at 15, 25, and 40 mm away from the epicenter on the top surface along the [010] direction, while the source was fixed on the bottom surface. Fig. 1 shows a focusing behavior of normalized intensity of the FT waves detected by the transducer positioned at 40 mm, where the position x represents the distance from the [010]-axis. Square of the peak amplitude immediately after the arrival of the FT mode was used as a measure of intensity. The 2 mm half-width of the approximately Gaussian curve makes 1.8°, viewed from the source. The focusing patterns obtained by the other two detectors are very similar to Fig. 1. Note good comparison of Fig. 1 with Fig. 2, which displays a theoretically obtained polar plot of the phonon focusing pattern of the FT mode, following the definition of the phonon enhancement or focusing factor given by Maris [7]. In Fig 2 the scan direction of the 40 mm

1051-0117/92/0000-1009 $1.00 © 1992 IEEE

position detector is marked by a bidirectional arrow.

A more detailed description of the FT focusing in silicon will be given elsewhere [8]. It would be quite interesting to see more focusing patterns of FT mode of other crystals such as copper and cesium bromide, which exhibit focusing patterns different from that of silicon.

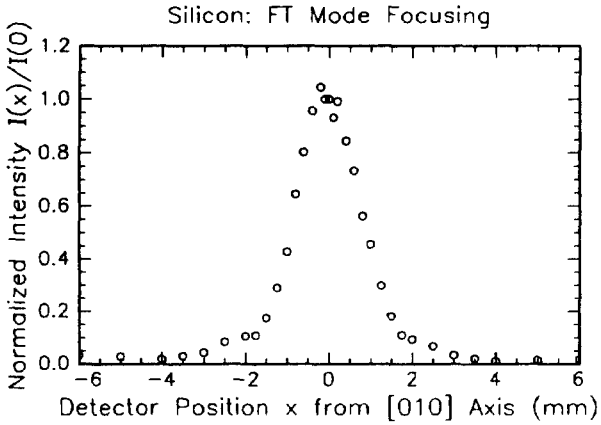

Fig. 1. Observed focusing pattern of FT mode in (001) silicon.

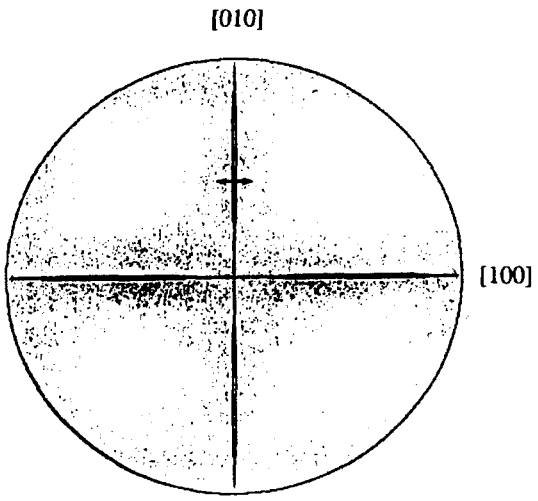

Fig. 2. Theoretical polar plot of FT mode focusing in (001) silicon. The bidirectional arrow shows a scan range.

III. DETERMINATION OF WAVE SURFACE OF ZINC

The treatment of the wave surfaces such as those of phase and group velocities, and of slowness of elastic waves, has been extensively given in literature [9]. Fig. 3 shows the (010) sections of slowness surface of zinc, those of longitudinal (L), FT and ST modes. In the figure the [001] direction represents the symmetry axis of a transversely isotropic zinc crystal, which is conventionally written as [0001] for a hexagonal crystal. The corresponding group velocity (or ray) surfaces are drawn as solid lines in Fig. 4. The values of elastic constants of zinc used to generate Figs. 3 and 4 were measured to be C_{11} = 163.75 GPa, C_{12} = 36.28 GPa, C_{13} = 52.48 GPa, C_{33} = 62.93 GPa, and C_{44} = 38.68 GPa. The cuspidal feature shown in Fig. 4 arises due to a peculiar shape of the ST mode slowness surface. It has a concave sheet around the symmetry axis , changes its curvature at point Q_c, and exhibits a convex surface on moving further outward with a gradient pointing parallel to the [001] direction at point Q_∞. In Fig. 4 the cuspidal edge and the branches of faster ST (FST), intermediate speed ST (IST), and slower ST (SST) modes, correspond respectively to the point Q_c and the sections of Q_aQ_c, Q_cQ_∞, and $Q_\infty Q_0$ on the ST slowness surface in Fig. 3.

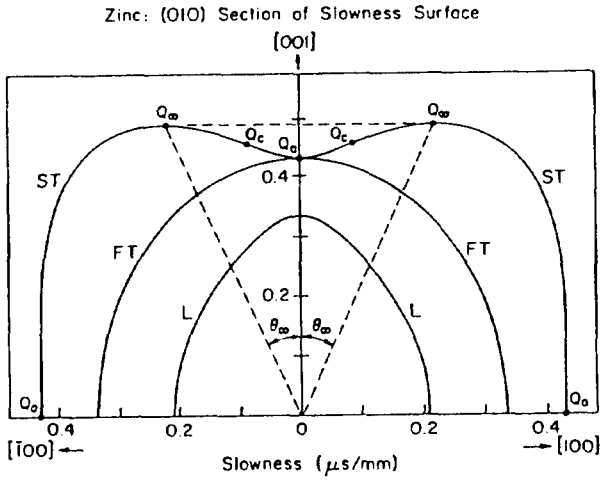

Fig. 3. (010) sections of slowness surfaces in zinc.

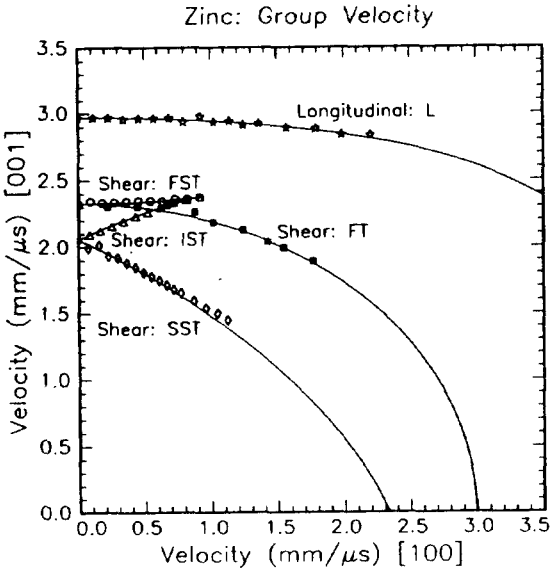

Fig. 4. Theoretical and measured group velocities in the (010) plane of zinc.

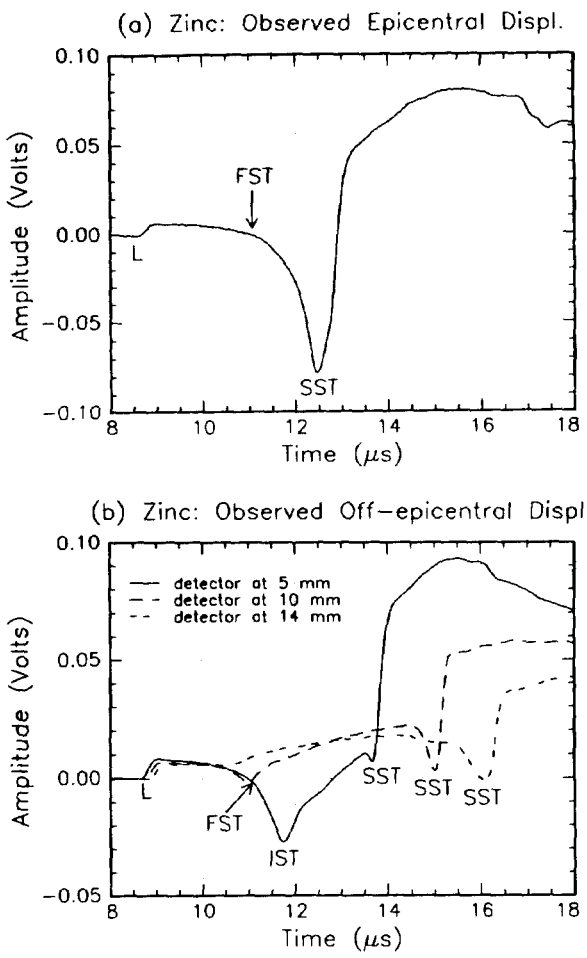

Fig. 5. (a) Epicentral displacement signal detected by a 1 mm capacitive transducer with a source of capillary fracture. (b) Off-epicentral displacement signals obtained with the same system.

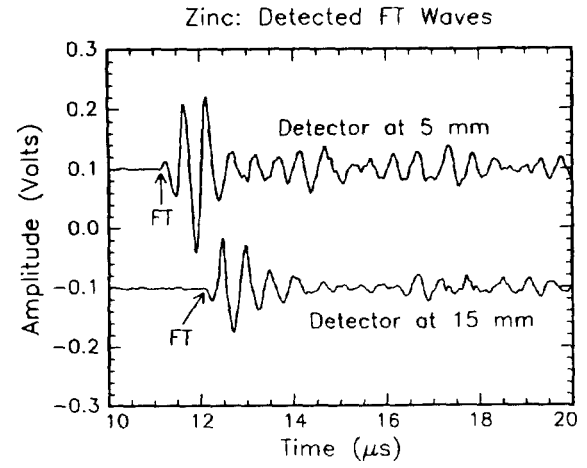

Fig. 6. FT waves detected by a small PZT shear transducer.

The group velocity data associated with the L, FST, IST and SST branches in Fig. 4 have been obtained from the waveforms detected by a capacitive displacement sensor located on the bottom surface of a disk-shaped zinc specimen with dimension of 25.7 mm in thickness and about 75 mm in diameter. The elastic waves were generated by the sudden fracture of a glass capillary when it was pressed vertically with a razor blade on the top surface of the specimen. This generated a axisymmetric source of vertical force drop whose time function resembles a Heaviside step with risetime less than 0.1 μs, and gave rise to only L and ST modes for the reasons mentioned in the previous section. Some of the detected waveforms are displayed in Fig. 5, where L indicates the arrival of the L mode. The epicentral signal of Fig. 5(a) shows the arrivals of FST and SST rays at the points of the first zero crossing and single sharp negative minimum, respectively. Fig. 5(b) indicates the arrivals of FST, IST, and SST rays at the points of the first zero crossing, the first negative minimum, and the second local minimum, respectively. In the figure the orientation from the source to the sensor located at 10 mm away from the epicenter approximately corresponds to the orientation of the cuspidal edge in Fig. 4. Note that outside the cuspidal edge (see 14 mm signal of Fig. 5(b)), both the zero crossing and the negative minimum, each corresponding to the arrivals of the FST and IST rays, respectively, disappear and only the SST ray arrival associated with the second minimum is distinctive after the L wave arrival.

The group velocities associated with the FT branch in Fig. 4 have been measured using two small PZT shear transducers. One transducer acted as a fixed source on the bottom side of a specimen and the other served as a variable position detector on the top surface. This is similar to the configuration adopted for the FT mode focusing described in the previous section. The two shear transducers had their polarizations aligned along the same direction in the transversely isotropic basal plane and the detector was moved along the direction perpendicular to the sagittal plane defined by the symmetry axis and the polarization direction. Only the FT mode of SH polarization was obtained. This was confirmed by the fact that no appreciable signal was detected when the detector was rotated by 90°. Two FT mode signals detected at 5 and 15 mm away from the epicenter are shown in Fig. 6. They are offsetted by ±0.1 volt for distinctive display.

Features of the wave surface such as the L, IST and SST branches are clearly visible in the scan image of the signal shown in Fig. 7. This was obtained when a focused laser beam scanned the top surface and a small PZT longitudinal transducer was used as a detector on the bottom side. Note that the head wave (HW) front is also distinctive and marked with HW in the figure. The laser beam generates a strong L mode propagating along the surface and it sheds part of its energy to the interior as a head wave. The ray direction of the head wave has a calculated azimuthal angle of -3.04° measured from the symmetry axis of zinc to the detector. Near the epicenter the arrivals of both SST and HW rays are almost simultaneous and so, both arrivals are therein indistinguishable. However, farther from the epicenter, they gradually diverge, as seen in Fig. 7. As mentioned before, the laser beam does not excite a

FT mode and the absence of FST mode in Fig. 7 is probably because the PZT detector is principally sensitive to the change of surface displacement which looks very weak at the arrival of the FST mode shown in Fig. 5.

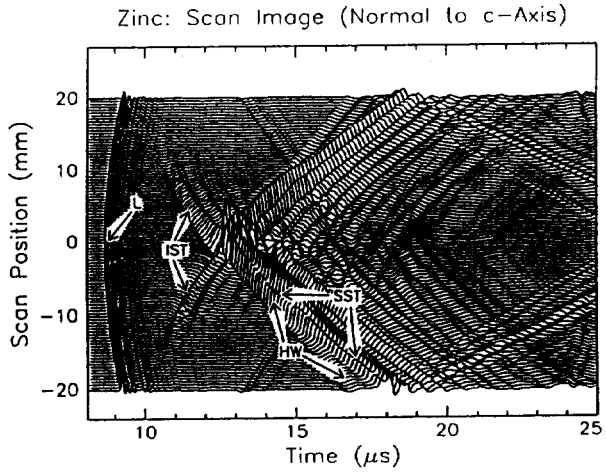

Fig. 7. Scan image of laser generated signals detected by a small longitudinal PZT transducer.

A more detailed description of the wave surface of zinc and the laser scan image will be published elsewhere [10].

IV. EXTERNAL CONICAL REFRACTION IN ZINC

A theoretical treatment of the external conical refraction (ECR) was given in some detail [9]. And yet, there has been, to our knowledge, no report of experimental observation of this phenomenon in acoustics. The ECR was claimed to be observed in optics [11]. Here we present convincing evidences for the observation of ECR in zinc.

Payton [12] calculated a vertical displacement response at a buried epicentral point due to an excitation of an axisymmetric Heaviside-step source acting vertically on the surface of a half-space, zinc crystal. Here the vertical direction coincides with that of the symmetry axis of zinc. The epicentral response obtained by Payton is shown in Fig. 8, where L, T_1, and T_2 respectively denote the arrivals of L, FST and SST waves. Fig. 8 plots the normalized displacement in units of $\rho F_3/(4\pi h C_{44})$ and the normalized time in units of the FST arrival time equal to $h/(C_{44}/\rho)^{1/2}$, where ρ, F_3, and h are the density of zinc, magnitude of Heaviside step force, and the distance from the source to the detector, respectively. The epicentral signal in Fig. 5(a), which corresponds to a specimen of plate geometry, should be similar to the Payton's curve shown in Fig. 8 and differs only in amplitude which depends on the reflection coefficient of a traction-free surface. Note strong similarity between these two signals. Deviation from similarity after 16 μs in the experimental signal is due to the reflections from the side wall of the specimen. The Payton's calculation predicts a negative singularity at the arrival of the SST ray. This is the result of focusing of ST rays toward the symmetry direction of zinc. These rays correspond to the ST modes associated with the conical section OQ_∞ with the azimuthal angle θ_∞ on the ST sheet of slowness surface shown in Fig. 3. In other words, all the energy of those ST modes whose wave normal vector k's are all parallel to the direction of OQ_∞ of the conical section on the ST slowness surface is directed to the epicentral, symmetry direction and give rise to the negative singularity at T_2 in Fig. 8. This result is evident in the epicentral waveform of Fig. 5, which shows a very sharp, large negative minimum at the corresponding point of SST ray arrival. The finite value of the negative minimum is due to the finite size of the sensor and finite bandwidth of the detection system.

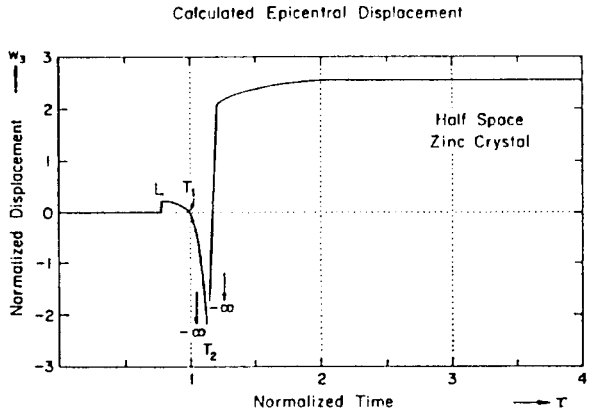

Fig. 8. Calculated epicentral displacement response for half space of zinc with a Heaviside step source.

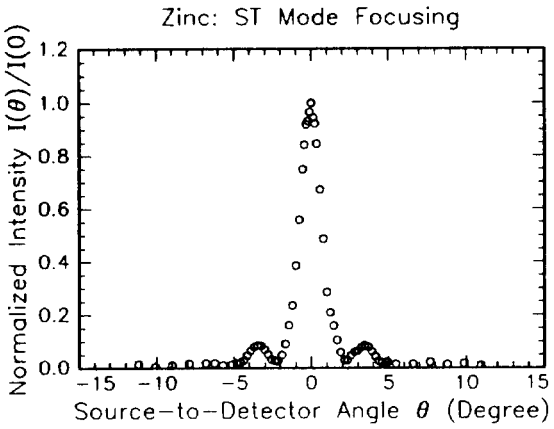

Fig. 9. Observed focusing pattern of ST mode in zinc.

The acoustic energy of the ST ray rapidly diminishes as the ray direction moves away from the symmetry direction. This is illustrated in Fig. 9 which shows a distribution of normalized intensity about the symmetry direction. Note the strong ST mode focusing toward the symmetry direction of zinc. This focusing pattern is in good agreement with Fig. 10 obtained theoretically by using the definition of phonon focusing factor [7], as in the case of the FT mode focusing in

silicon. In Fig. 10 the intense central spot and the circumference of a large circle correspond to the directions of symmetry and the cuspidal edge shown in Fig. 4, respectively. The direction of the cuspidal edge is calculated to be 21.5° from the symmetry axis. The azimuthal angle θ in Fig. 9, which indicates a source-to-detector orientation, is also measured from the symmetry direction. A longitudinal PZT transducer fixed at the center of the bottom surface acted as a source and a L mode PZT detector was scanned across the epicentral, symmetry direction on the top surface to detect the waves of L and ST modes. Again, square of peak amplitude immediately after the arrival of SST ray is used as a measure of intensity in Fig. 9.

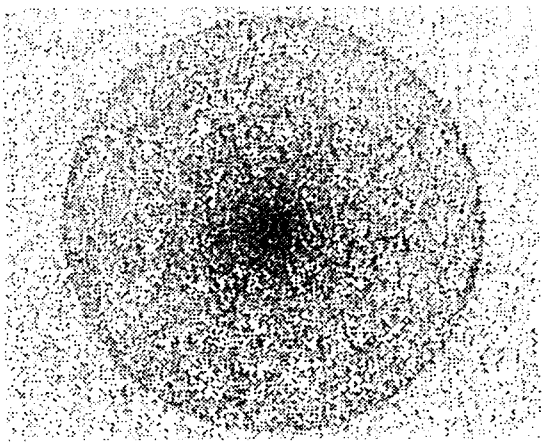

Fig. 10. Calculated focusing pattern of ST mode in zinc

The wavefront of the focused ST ray traveling along the symmetry axis of zinc is nonplanar. As a result, when this ST ray is transmitted through the planar boundary to an isotropic medium such as glass or polycrystalline aluminum, it is refracted into an array of cones instead of along single conical surface. Detailed version of this external conical refraction will be reported elsewhere [13].

ACKNOWLEDGMENT

We deeply appreciate the financial support of the Physical Acoustics Division of the Office of Naval Research. We are also indebted to professor Arthur Every at the University of the Witwatersrand, South Africa for his many illuminating suggestions and discussions.

REFERENCES

1. C.H. Palmer, R.O. Claus, and S.E. Fick, *Appl. Opt.* **16**, 1849 (1977).

2. K.Y. Kim, L. Niu, B. Castagnede, and W. Sachse, *Rev. Sci. Instrum.* **60**, 2785 (1989).

3. B. Taylor, H.J. Maris, and C. Elbaum, *Phys. Rev. Lett.* **23**, 416 (1969).

4. A.G. Every, W. Sachse, K.Y. Kim, and M.O. Thompson, *Phys. Rev. Lett.* **65**, 1446 (1990).

5. M.R. Hauser, R.L. Weaver, and J.P. Wolfe, *Phys. Rev. Lett.* **68**, 2604 (1992).

6. A.A. Kolomenskii and A.A. Maznev, *Jetp. Lett.* **53**, 423 (1991).

7. H.J. Maris, *J. Acoust. am.* **50**, 812 (1971).

8. K.Y. Kim, A.G. Every, and W. Sachse, sub. to *Phys. Rev. Lett.*

9. M.J. P. Musgrave, *Crystal Acoustics*, Holden-Day, San Francisco (1970).

10. K.Y. Kim and W. Sachse, sub. to *J. Acoust. Am.*

11. M. Born and E. Wolf, *Principles of Optics*, 6th Ed., Pergamon Press, New York (1980).

12. R.G. Payton, *Elastic Wave Propagation in Transversely Isotropic Media*, Martinus Nijjhoff, Hague (1983).

13. K.Y. Kim, A.G. Every, and W.Sachse, sub.to *J. Acoust. Soc. Am.*